J. Astrophys. Astr. (September 2017) 38:53
DOI 10.1007/s12036-017-9462-9

Review

Nulling, Mode-Changing and Drifting Subpulses in the Highly Asymmetric Conal Quadruple Radio Pulsar B2034+19

JOANNA M. RANKIN

Physics Department, University of Vermont, Burlington, VT 05405, USA.
E-mail: Joanna.Rankin@uvm.edu

MS received 13 April 2017; accepted 24 July 2017; published online 12 September 2017

Abstract. Radio pulsar B2034+19 exhibits all three 'canonical' pulse-sequence phenomena—that is, pulse nulling, two distinct profile modes and subpulses with periodic modulation. Indeed, the bursts and nulls in the pulsar are short at several score pulses and quasi-periodic such that about 1/3 of the pulses are nulls. The pulsar's two modes have very different characteristics, the first shows emission almost completely confined to the leading half of the profile and highly modulated in a 2-period odd–even manner; whereas the second mode illuminates both the leading and trailing parts of the star's profile about equally with the appearance of drift bands at about a 3-period separation. The second mode occurs much less frequently than the first (about 15% of the time) and thus the leading part of the profile has a much larger average intensity than the trailing part. B2034+19 represents an interesting example of a pulsar with emission primarily in the leading part of its profile window with only occasional illumination in the trailing part. This suggests that there are pulsars that perhaps never emit in a part of their profile window, connecting with earlier work on pulsars with apparent 'partial cone' profiles.

Keywords. Pulsars: general—individual (B2034+19).

1. Introduction

Radio pulsar B2034+19 is a moderately bright slow pulsar in the Arecibo sky, which shows all three canonical pulse-modulation phenomena of pulse nulling, mode-changing and subpulse drifting. Its discovery was announced by Stokes *et al.* (1985) who had conducted a *survey for short period pulsars*—that disappointingly identified no really fast pulsars among their 20 new objects. Apparently the pulsar is too weak for most instruments as it appears in neither the extensive Jodrell Bank polarization survey of Gould and Lyne (1998) nor the Westerbork fluctuation-spectral surveys of Weltevrede *et al.* (2006, 2007). It does appear in the Arecibo polarimetric surveys at 21 cms (Weisberg *et al.* 1999) and 430 MHz (Weisberg *et al.* 2004) as well as the more recent GMRT (Gajjar *et al.* 2012) and LOFAR (Bilous *et al.* 2016) surveys.

Pulsar B2034+19 first attracted our attention because the trailing part of its profile shows substantial variability—just as did the first pulsars identified as exhibiting the mode-switching phenomenon. Pulse sequences showed bursts of several tens of pulses interspersed with null intervals of similar duration. Closer inspection revealed pulse modulation of two different kinds: (a) intervals of nearly odd–even counter-phase modulation in the two bright leading components, and (b) shorter episodes of apparent subpulse drift, usually extending across the entire profile, with a drift band spacing of about 3 rotation periods (hereafter P_3).

The pulsar is typical of many others in having an estimated surface magnetic field of some 2×10^{12} G and an age of roughly 10 Myr—and is relatively local with a DM of 36 pc/cm^2 and distance of just over 2 kpc. However, its 2.074 s rotation period (hereafter P_1) is substantially slower than most pulsars, and its spin-down energy of 9×10^{30} ergs/s falls in the lowest 10% of all known radio pulsars. As the three canonical phenomena above are associated with slower pulsars, we have wondered if it could in part stem from their smaller polar caps and flux tubes. In this paper, we explore these questions in the context of observations of pulsar B2034+19. Section 2 describes the available Arecibo observations, section 3 discusses the pulsar's profile,

Table 1. Observations.

Band	MJD	BW (MHz)	Resolution (°)	Pulses (#)
P	52949	25	0.36	629
P	53377	25	0.36	1676
P	56353	50	0.36	2048
P	56415	50	0.35	1915
L	52735	400	0.18	289
L	56285	350	0.26	1334
L	56564	350	0.30	1341

beam form and sightline geometry, and section 4 its pulse-sequence modulation. Section 5 gives a summary and discussion of the implications of this work.

2. Observations

The observations were carried out using the upgraded Arecibo Telescope in Puerto Rico with its Gregorian feed system, 327 MHz (P band) or 1100–1700 MHz (L band) receivers, and Wideband Arecibo Pulsar Processors (WAPPs) or the Mock Spectrometers. At P band, a single WAPP was used for the 25 MHz observations, and four Mocks sampling of 12.5 MHz bands were used across the 50 MHz bandpass available later. Four nominally 100 MHz bands centered at 1170, 1420, 1520 and 1620 MHz were used at L band, and the lower three were usually free enough of radio-frequency interference (hereafter RFI) such that they could be added together to provide about 300 MHz bandwidth nominally at 1400 MHz. The four Stokes parameters were formed off-line in software, corrected for interstellar Faraday rotation, various instrumental polarization effects and dispersion. The instrumental resolutions of the observations are all about a milliperiod. The Modified Julian Dates (MJDs) as well as the resolutions and lengths of the observations are listed in Table 1. Slow pulsars with small dispersion measures are more subject to RFI than those of faster, more dispersed pulsars, so we have had difficulty avoiding or removing the RFI from the pulse sequences used here.

3. Profile, beamform and sightline geometry

3.1 *Profile characteristics*

The radio beamforms and sightline-traverse geometry of most slow pulsars can be understood in terms of a core/double-cone emission-beam model (e.g., Rankin 1993a, hereafter ET VIa). However, no one looking at the profile of B2034+19 could have understood it in these terms without substantially more information about its single-pulse behavior. Therefore, the star remained essentially unclassifiable in terms of this model—i.e., do either of its two bright peaks represent a core component? Which features might represent leading or trailing conal components, etc.?

High quality polarimetric profiles of B2034+19 were measured by Weisberg *et al.* (1999, 2004; their figures 24 and 20, respectively) with an intent of providing morphological classifications; however, the profiles at the two bands appeared to indicate such different types of beamforms, that no clear understanding emerged. We are now able to make even higher quality Arecibo observations as outlined in Table 1; however, the 327 and 1400 MHz profiles on their own do little more to resolve questions about the pulsar's beamform and geometry.

Our 325 MHz profile is shown in Fig. 1 and the asymmetry between the bright leading pair of components and the single trailing 'bump' is striking. Such a form corresponds to none of the profile classes outlined in ET VIa. What we do see are two trailing regions with different orthogonal linear polarization angles (hereafter PPAs), a relatively strong one at about +3.5° longitude and a weak one near +6°. The leading component shows populations of two orthogonal PPAs which strongly depolarize it, while the second component is less so depolarized, showing high fractional linear on its trailing edge—all typical characteristics of leading outer and inner conal components in profiles where both cones are present.

Importantly, Fig. 1 also shows a PPA track connecting the leading and trailing parts of the profile. Its total rotation is a little more than 90°, its inflection point near the center of the profile, and its slope is estimated at about +29±3°/°. The earlier polarimetry fails to show this PPA traverse clearly, and having a clear estimate of its central slope and total traverse is necessary for understanding the pulsar's beamform quantitatively. The steep slope and traverse through more than 90°, but significantly less than 180°, indicates an intermediate sightline path that is neither central (i.e., close to the star's magnetic axis), nor fully oblique.

Clarification about the form of the pulsar's profile comes strongly from a recent survey of pulsars detected using the high band of the LOFAR telescope in the Netherlands. This profile of B2034+19 is shown in Fig. 2, and its four well-resolved components are obvious. Interestingly here, the profile is highly asymmetric in terms of intensity but the two pairs of putative conal

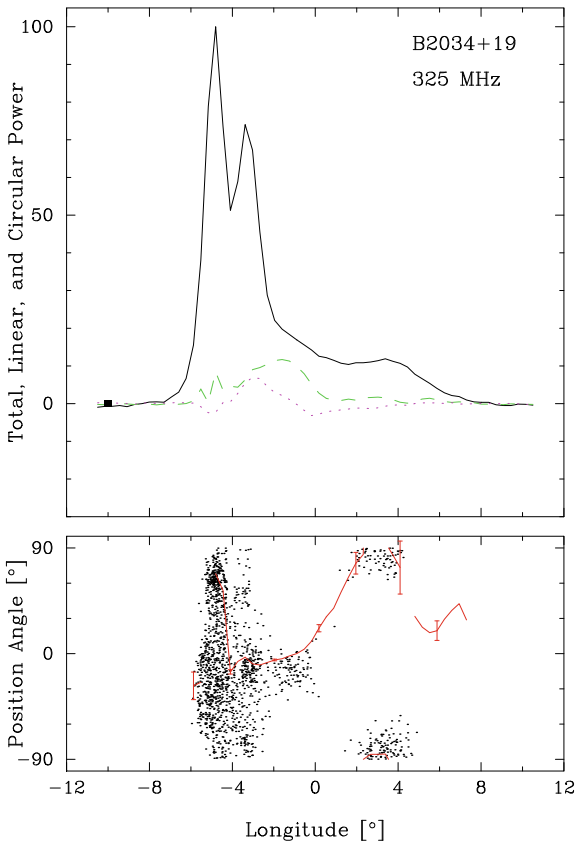

Figure 1. The two panels display the relative total power (Stokes I), total linear polarization (L [=$\sqrt{Q^2+U^2}$]; dashed green) and circular polarization (Stokes V, defined as left-hand–right-hand circular polarization; dotted magenta) (*upper*), and the polarization angle (PPA [=$\frac{1}{2}\tan^{-1}(U/Q)$]) (*lower*). Individual samples that exceed an appropriate >2 sigma threshold appear as dots with the average PPA (red curve) overplotted. The small box at the left of the upper panel gives the resolution and a deflection corresponding to three off-pulse noise standard deviations.

components are nearly symmetrical in their longitude spacing.

The pulsar then seems to have a profile of the conal quadruple (c**Q**) class (ET VIa) wherein the sightline encounters both cones centrally enough to resolve them but also misses any central core-component emission. Profiles of this type are rare as might be expected because a more central sightline cut would encounter the core to give five components and a less central traverse would not resolve the inner cone into two well separated components. Only a few other such pulsars are known, and their similarities and differences will be discussed below. In the next subsection, we will explore the pulsar's quantitative geometry in order to assess whether the beamforms and sightline traverse are compatible with the c**Q** classification.

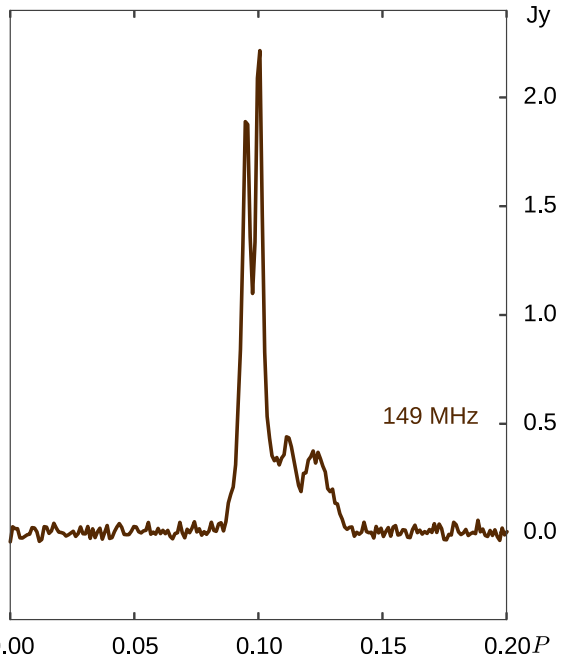

Figure 2. Total power LOFAR profile of B2034+19 at 149 MHz from Bilous *et al.* (2016; their Fig. 23). Note the highly asymmetric profile in terms of amplitude, with four well resolved components symmetric in longitude with respect to the profile centre. The longitude scale is given in period units or phase such that an interval of 0.05 represents 18°.

3.2 *Quantitative geometry*

Slow pulsars with four-component profiles show outer and inner pairs of conal components, centered closely on the (unseen) longitude of the magnetic axis, all with particular dimensions relative to the angular size of the pulsar's (dipolar) magnetic polar cap. The classes of pulsar profiles and their quantitative beaming geometries are discussed in Rankin (1983, ET I) and Rankin (1993a,b, ET VI), and other population analyses have come to similar conclusions (e.g., Gil *et al.* 1993; Mitra & Deshpande 1999, Mitra & Rankin 2011). A pulsar's polar cap has a (dipolar) angular diameter of $2.45^\circ P_1^{-1/2}$, and the outside half-power conal beam radii of the slow pulsars also scale as 4.33 and $5.75 P_1^{-1/2}$ respectively, and reflect emission from characteristic heights of one or two hundred kilometres.

Following the practice in ET VIa, a spherical geometric model is used to estimate the conal beam radii of the inner and outer cones corresponding to the two pairs of conal components in B2034+19. These measurement are given in Table 2 that were possible for the three available frequencies. Understandably, the dimensions of the outer cone are more easily estimated than

Table 2. Conal geometry model for B2034+19.

	Inner cone		Outer cone		Height (km)	
Frequency (MHz)	w (°)	ρ (°)	w (°)	ρ (°)	Inner	Outer
1400	–	–	9.5	4.0	–	222
327	7.6	3.4	11.3	4.6	160	293
149	5.8	2.9	12.2	4.9	114	333

Note: α is equal to 47°, and β to 1.9°

the inner one which can only be seen clearly at the lowest frequency. Equation (3) in ET VIa is used to relate the sightline impact angle β to the magnetic co-latitude α; equation (4) in ET VIa is then used to compute the conal radii and equation (5) in ET VIa is used to estimate the characteristic emission heights. The results of the modeling in Table 2 show that a consistent double-cone model is reasonable for B2034+19: for an α value of about 47°, the inner and outer conal characteristic heights are around 130 and 220 km, respectively. Moreover, the outer cone's radius is seen to increase with wavelength as do all known outer cones. Finally, the core-component half-power radius, if present, would only be 0.85°, so the 1.9° impact angle would largely miss it, though the center of the star's profiles have space to accommodate a weak core feature if present.

4. Pulse-sequence dynamics

Pulsar B2034+19 is just bright enough with benefit of Arecibo's large sensitivity to study its polarized pulse sequences, and a colour-coded display of a typical 200-pulse interval is given in Fig. 3. Here, we can readily see what will be studied in more detail in the following subsections: (a) about 1/3 of the pulses are nulls, typically about 10 pulses in duration; (b) the individual pulses obviously exhibit two modes, one with emission confined to the early part of the profile and a second wherein bright emission extends over the full profile width; and (c) the two modes show two distinct types of subpulse modulation or 'drift', an even–odd modulation in the first mode and clear drift bands in the other mode.

4.1 *Nulling behavior*

That B2034+19 exhibits frequent nulls is obvious from the 200-pulse display of its polarized pulse sequence in Fig. 3. Moreover, one is given the impression that there is a pattern to the pulsar's bursts and nulls. In order to explore the properties of these bursts and nulls, we first compute a null/burst histogram, and this is plotted in Fig. 4. Immediately we see that about 1 in every three pulses is a null[1] rather than 0.2. Herfindal & Rankin (2009) mentioned 44% but this reflects both a different technique and the shorter pulse sequences then available. Gajjar *et al.* (2012) obtained a lower limit of 26% perhaps reflecting a bit smaller signal-to-noise ratio. The off-pulse baseline of this observation is curved because of RFI, so the null distribution is off-centered a little and the off-pulse noise distribution is broader than the null distribution. We also see that the burst distribution is only somewhat skewed, showing that the bursts have a fairly consistent intensity with only a small population of stronger pulses in the second mode—to say nothing about RFI!.

We also computed null- and burst-length histograms, but this analysis was not very informative as the individual-pulse signal-to-noise ratio is only marginal for distinguishing pulses from nulls, so that the distributions are dominated by 1-period events many of which are incorrectly identified.

Instead, we discovered that B2034+19's longitude-resolved fluctuation spectra (lrfs) show strong periodicity, and that this periodicity is primarily due to the burst-null-interval modulation. When so analysed using 128-length Fourier transforms, two of our observations show primary peaks at a $64\,P_1$ modulation and the third (MJD 56415) peaks at $43\,P_1$. Though due to the $\pm 16\,P_1$ error the difference is insignificant, suggesting that the actual value falls somewhere intermediate. The analysis for MJD 56353 is shown in Fig. 5, where the top display gives the lrfs and the lower one the 17-bin modulation-period-folded pulse sequence. Note the deep minimum in the folded display, where there is about a factor of two of intensity variation around the modulation cycle. The other two observations behave almost identically, save for the different modulation peak as above.

What is important is that the sequences of bursts and nulls in B2034+19 exhibit a 40–60-pulse quasi-periodicity such that the bursts tend to have lengths of 25–40 pulses and the nulls 15–20 pulses. The physical origin of this periodicity is unclear. However, the evident quasi-periodicity squares with a RUNS-test value of some −25 (Redman & Rankin 2009) indicating that the nulls are non-random in a heavily 'undermixed' manner—though the interpretation of the Wald–Wolfowitz RUNS test may be more complicated depending on the physical model involved as discussed by Gajjar *et al.* (2012) and Cordes (2013).

[1] The precise null fraction is difficult to determine accurately. The 36% in Fig. 4 could be larger by a few percent if, for instance, the threshold was taken at 0.3 $I/\langle I\rangle$.

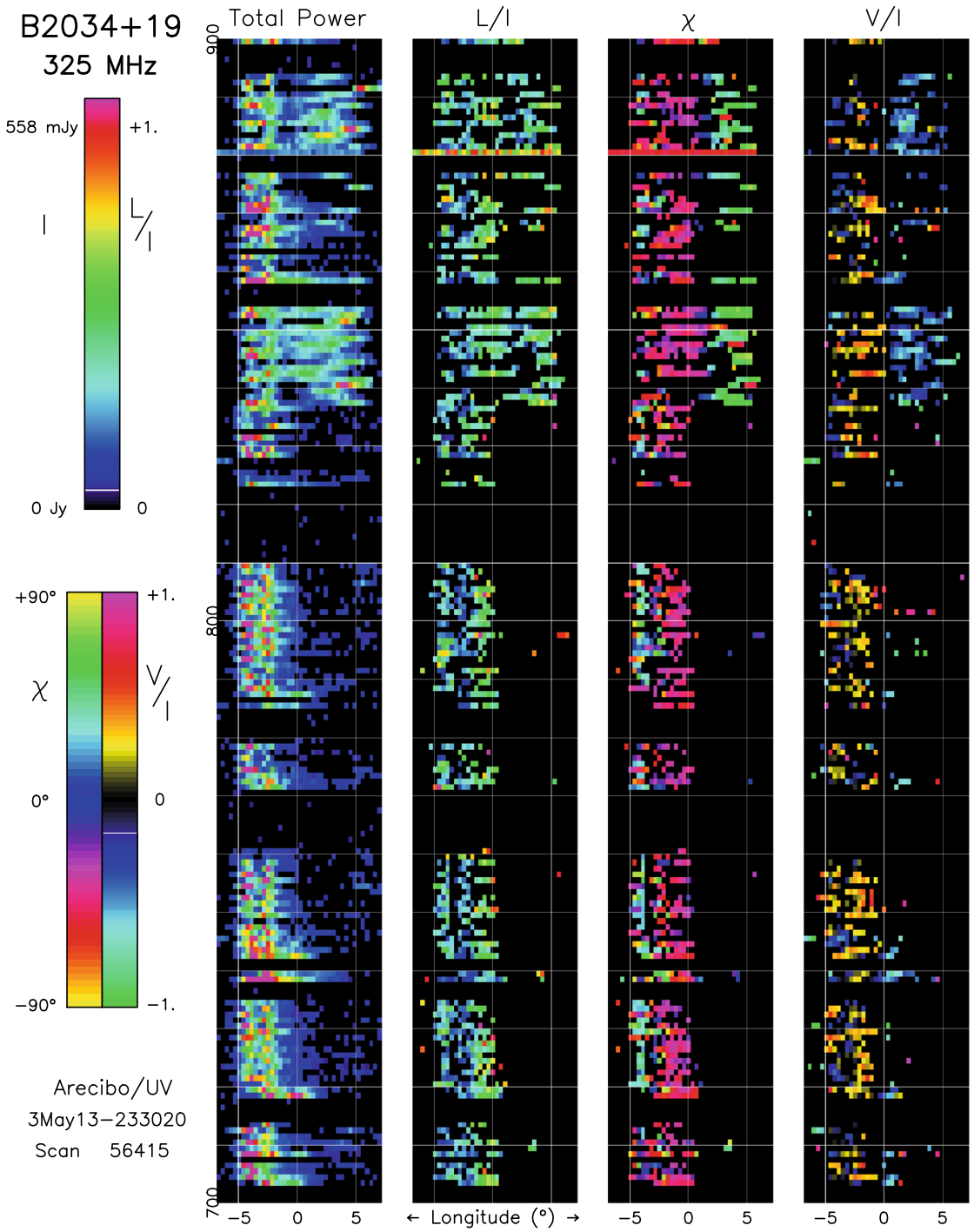

Figure 3. Pulse-sequence polarization display showing several of the pulsar's PS behaviors. The first 120 or so pulses (700–820) show a series of short bursts and nulls, where the pulsar is in its first mode characterized by emission almost entirely within the leading half of its profile. Here the subpulse modulation is odd–even and stationary within the two bright components. The last (upper) portion of the display shows the pulsar in its less than usual second mode where emission occurs with comparable intensity in both the leading and trailing parts of its profile. In this second mode, one can also see that the pulse modulation is very different with a roughly 3-period pattern and the suggestion of drift bands extending across the full profile width. This second mode occurs during only about 15% of the star's bursts and its rarity along with the restricted longitude reach of the first mode is responsible for the extreme asymmetry of the star's profile. The total power I, fractional linear L/I, PPA χ, and fractional circular polarization V/I are colour-coded in each of four columns according to their respective scales at the left of the diagram. The 3-σ background noise level of this sequence is indicated by the white stripe within the lowest intensity black portion of the I color scale.

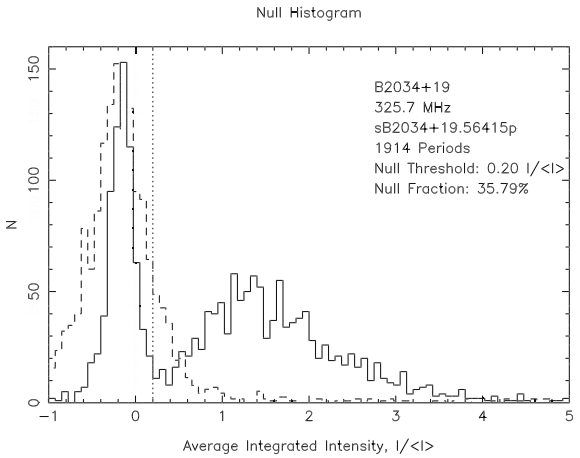

Figure 4. Null histogram for B2034+19's MJD 56415 P-band 1914-pulse sequence. The null fraction confirms that about a third of the star's pulses are nulls. It also shows that the emitted pulses are relatively constant in intensity as they show little high intensity 'tail'. This and our other observations have uneven off-pulse baselines, which is why the off-pulse peak is not centered at zero and the off-pulse noise distribution has a larger variance than the nulls.

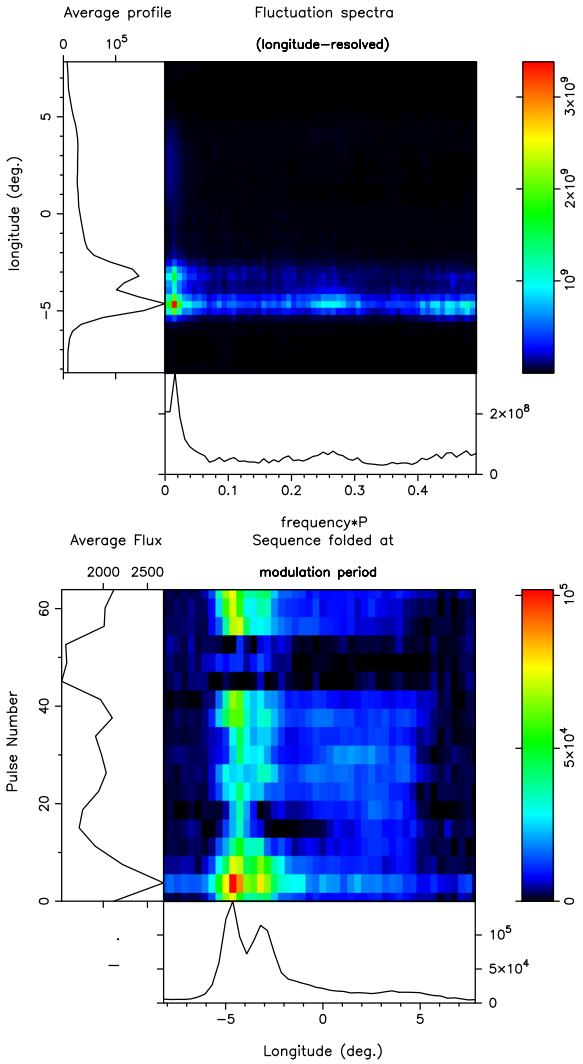

Figure 5. Longitude-resolved fluctuation spectra (lrfs) for B2034+19's MJD 56353 P-band 2048-pulse sequence (*top*) and a display of the observation folded at the fluctuation-spectrum peak of 64 P_1 (*bottom*). The average profile is shown at the left corresponding to the spectra in the central panel with the integral spectrum in the lower panel. The strong single peak in the 128-point lrfs is responding primarily to the burst-null modulation of the sequence, and when folded (using 17 bins) at this period the intensity shows deep crenelation around the modulation cycle (left panel). The bottom panel shows the 'base' profile that is subtracted from the central display.

4.2 *Two distinct modes*

Pulsar B2034+19's two distinct modes are obvious in Fig. 3. Most of the single pulses illuminate only the early part of the profile, whereas other intervals have bright emissions extending over the full profile. This is the cause of the pulsar's highly asymmetric average profile. Reference to the upper parts of Fig. 3 show short sequences in which emission in the trailing profile is about as strong as that in the leading region. Therefore, the ratio of intensities in the leading and trailing regions of the average profiles gives a fairly accurate indication of the modal ratio. Fig. 1 indicates a peak intensity at about +3° longitude of about 15% that of the first component. We can then say with confidence that the second mode occurs in about 15% of the burst pulses. In Fig. 3, there are some 130–140 pulses, and 25–30 of these show the full width of emission characteristic of the second mode.

4.3 *Drifting subpulse patterns*

The first mode shows no clear drift, but it seems always to show a strong odd–even modulation. This is very clear in Fig. 3, and moreover emission in the second component always seem to be out of phase with bright subpulses in the first component. Fluctuation spectra of several total sequences do not pick up this modulation because they are dominated by the burst-null fluctuations. However, we computed an artificial sequence in which the nulls were removed in Fig. 6, and this shows a strong feature at about 0.46 cycles/P_1 or a cycle of nearly 2 periods. This modulation is confined narrowly to the positions of the two leading profile components and thus appears to be nearly pure amplitude modulation.

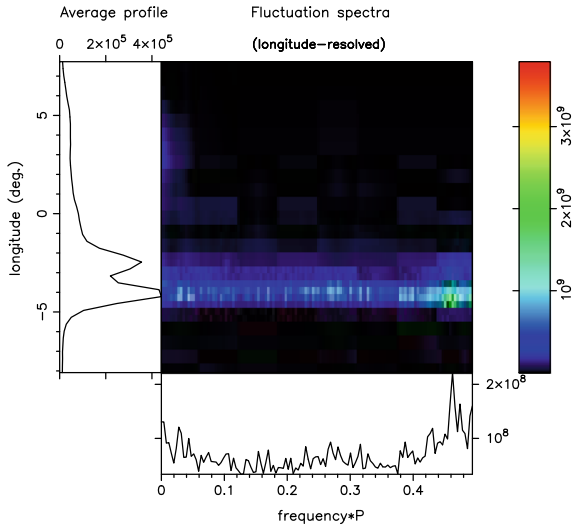

Figure 6. Lrfs for B2034+19's MJD 56415 P-band 1914-pulse sequence with the null pulses removed. The remaining 1391 pulses then exhibit no low frequency feature but do show a strong feature produced by the odd–even modulation of the dominant mode. Overlapping 256-length transforms were used to compute the spectra.

The second mode gives more of an appearance of drift, but its apparitions are so brief in our observations that it is difficult to discern fully what is happening. Its modulation is clearly very different than the first mode with emission bands spaced at 3 or $4P_1$ intervals; however, we found no interval in any of our AO observations where the second mode persisted for more than 15–20 pulses, so we could not use fluctuation spectra to study this second mode in detail. Note in Fig. 3 that the second mode seems to cross the profile in steps as if amplitude modulating the pair of trailing components.

5. Discussion

Pulsar B2034+19 provides a further interesting example of an object showing all three of the 'canonical' pulse modulation effects, pulse nulling, multiple profile forms associated with different 'states' of subpulse activity as well as systematic subpulse modulation or 'drift' associated with each mode. We find that about one-third of B2034+19's pulses are nulls and that these occur in a quasi-periodic manner in burst-null cycles typically 45–60 pulses long. In several observations, we never see bursts longer than about 40 pulses. The star's pulse sequences also show strong moding with a usual behaviour in which emission is confined to the leading half of the average profile—thus the two strong leading components, and a second less frequent mode where both the front and back of the profile are illuminated about equally. The first mode is characterized by a regular odd–even subpulse modulation in which the first and second components appear in counterphase; whereas the brief apparitions of the second mode show systematic modulation across the full width of the profile in the form of drift bands with an approximate $3P_1$ separation.

B2034+19 is identified here as having a conal quadruple (c**Q**) class profile (ET VIa) wherein the sightline encounters both cones centrally enough to resolve them but also misses any central core-component emission. Our geometric model of the pulsar's emission beam estimates α at about 47° and β at 1.9°.

A few other pulsars with c**Q** class profiles have been identified. Double cones are overall unusual with many more pulsars exhibiting an outer cone or an inner cone, but not both. **cQ profiles** are further unusual because they reflect a very particular sightline geometry which has β large enough to miss the core (as in the five-component **M** class) but small enough that the sightline resolves both cones (lest the profile instead have a conal triple c**T** form).

A few other pulsars with conal quadruple profiles are known. A polarized profile for pulsar B2003–08 was given by Lyne & Manchester (1988; their fig. 2), and they also discuss the important question of partial cone emission, which we further consider below. ET VIb lists a number more, some of which unsurprisingly are difficult to distinguish from conal triple (c**T**) pulsars: e.g., B1633+24, the first Cambridge pulsar B1919+21, B2315+21 and B2319+60. In particular, an extensive study of pulsar B1944+17 (Kloumann & Rankin 2010), found that the pulsar's profile represented something of a hybrid between the c**T** and c**Q** classes and that the pulsar had an unusual sightline traverse that lay entirely within the pulsar's beam.

While ETI wondered if pulsars with asymmetric single profiles such as B0540+23, B0611+22 and also B1915+13 might actually be 'partial' in the sense that a mirror part was not emitted, Lyne & Manchester (1988) assembled a list of stars that were either difficult to classify or showed evidence of being 'partial cones'. In an extensive pulse-sequence polarimetric study of these pulsars combining Arecibo and GMRT observations, Mitra & Rankin (2011) found some additional interesting examples of pulsars similar to B2034+19. Pulsar B1910+20 seems nearly a twin to B2034+19 but may show emission across its entire profile more consistently (see Fig. 2 of Mitra & Rankin 2011) and would certainly warrant further study in its own right. B0138+59 seems to have an almost mirror image profile where

its trailing region is regularly illuminated and its leading half much less so. Finally, B0450+55 appears to be a clear example of a partial cone where the leading region is illuminated but its trailing almost never so.

Similarly, there is considerable evidence that pulsars with profiles produced by 'skirting' oblique sightline traverses across the edge of the conal beam are asymmetric, and very often so with strong early and weak late emission within the profile 'window'. This was noted in ET VIa,b where many conal single ($\mathbf{S}_d$) pulsars seemed narrower than expected on the basis of their more resolved double forms at lower frequencies. The same issue was encountered in the ET IX analysis of Lyne & Manchester's 'partial cones' where about 25% of the objects considered could be identified as probable $\mathbf{S}_d$ stars with only partial filling of their emission window.

The paragon of drifting/moding pulsars, B0943+10 (Deshpande & Rankin 1999, 2001; Hermsen *et al.* 2013) exhibits the above issues with crystal clarity—and even dynamically. At meter wavelengths and above its usual $\mathbf{S}_d$ profile is well narrower that its 'window' with most emission coming in the leading region prior to the longitude of the magnetic axis. However, just after onsets of its drifting 'B' mode, the pulsar's profile has a well resolved conal double (**D**) form with the trailing component even somewhat brighter than the leading one. However, within a characteristic time of about an hour, the trailing component slowly diminishes in intensity, leaving the leading feature with its usual $\mathbf{S}_d$ form—as a sometime 'partial cone'.

Clearly such 'almost partial cone' pulsars as B2034+19 and its near relatives have much to teach us about how pulsars generate the plasma and the coherence necessary to emit the radio radiation we receive from them.

Acknowledgements

Much of the work was made possible by support from the US National Science Foundation Grant 09-68296 as well as NASA Space Grants. Arecibo Observatory is operated by SRI International under a cooperative agreement with the US National Science Foundation, and in alliance with SRI, the Ana G. Méndez-Universidad Metropolitana, and the Universities Space Research Association. This work made use of the NASA ADS astronomical data system.

References

Bilous, A. V., Kondratiev, V. I., Kramer, M., Keane, E. F., Hessels, J. W. T., Stappers, B. W., Malofeev, V. M., Sobey, C., Breton, R. P., Cooper, S., Falcke, H., Karastergiou, A., Michilli, D., Oslowski, S., Sanidas, S., ter Veen, S., van Leeuwen, J., Verbiest, J. P. W., Weltevrede, P., Zarka, P., Griessmeier, J.-M., Serylak, M., Bell, M. E., Broderick, J. W., Eisl"offel, J., Markoff, S. Rowlinson, A. 2016, *A&A*, **591**, A134.

Cordes, J. M. 2013, *ApJ*, **775**, 47.

Deshpande, A. A., Rankin, J. M. 1999, *ApJ*, **524**, 1008.

Deshpande, A. A., Rankin, J. M. 2001, *MNRAS*, **322**, 438.

Gajjar, V., Joshi, B. C., Kramer, M. 2012, *MNRAS*, **424**, 1179.

Gil, J. A., Kijak, J., Seiradakis, J. M. 1993, *ApJ.*, **272**, 268.

Gould, D. M., Lyne, A. G. 1998, *MNRAS*, **301**, 235.

Herfindal, J. L., Rankin, J. M. 2009, *MNRAS*, **393**, 1391.

Hermsen W., Hessels J. W. T., Kuiper L., van Leeuwen J., Mitra D., de Plaa J., Rankin, J. M., Stappers B. W., Wright G. A. E., Basu R. *et al.* 2013, *Science* **339**, 436.

Kloumann, I. M., Rankin, J. M. 2010, *MNRAS*, **408**, 40.

Lyne, A. G., Manchester, R. N. 1988, *MNRAS*, **234**, 477.

Mitra, D., Deshpande, A. A. 1999, *A&A*, **346**, 906.

Mitra, D., Rankin, J. M. 2011, *ApJ*, **727**, 92. (ET IX)

Rankin, J. M. 1983, *ApJ*, **274**, 359. (ET I)

Rankin, J. M. 1993a, *ApJ*, **405**, 285. (ET VIa)

Rankin, J. M. 1993b, *ApJ Suppl.*, **85**, 145. (ET VIb)

Redman, S. R., Rankin, J. M. 2009, *MNRAS*, **395**, 1529.

Stokes, G. H., Taylor, J. H., Weisberg, J. M. Dewey, R. J., 1985. *Nature*, **317**, 787.

Weisberg, J. M., Cordes, J. M., Kuan, B., Devine, K. E., Green, J. T. Backer, D. C. 2004, *ApJ Suppl.*, **150**, 317.

Weisberg, J. M., Cordes, J. M., Lundgren, S. C., Dawson, B. R., Despotes, J. T., Morgan, J. J., Weitz, K. A., Zink, E. C., Backer, D. C. 1999, *ApJ Suppl.*, **121**, 171.

Weltevrede, P., Stappers, B. W., Edwards, R. T. 2006, *A&A*, **445**, 243.

Weltevrede, P., Edwards, R. T., Stappers, B. W. 2007, *A&A*, **469**, 607.